

RESEARCH ARTICLE

Warmer, faster, stronger: Ca^{2+} cycling in avian myocardiumTatiana S. Filatova^{1,2,*}, Denis V. Abramochkin^{1,2,3,4} and Holly A. Shiels⁵

ABSTRACT

Birds occupy a unique position in the evolution of cardiac design. Their hearts are capable of cardiac performance on par with, or exceeding that of mammals, and yet the structure of their cardiomyocytes resembles those of reptiles. It has been suggested that birds use intracellular Ca^{2+} stored within the sarcoplasmic reticulum (SR) to power contractile function, but neither SR Ca^{2+} content nor the cross-talk between channels underlying Ca^{2+} -induced Ca^{2+} release (CICR) have been studied in adult birds. Here we used voltage clamp to investigate the Ca^{2+} storage and refilling capacities of the SR and the degree of trans-sarcolemmal and intracellular Ca^{2+} channel interplay in freshly isolated atrial and ventricular myocytes from the heart of the Japanese quail (*Coturnix japonica*). A trans-sarcolemmal Ca^{2+} current (I_{Ca}) was detectable in both quail atrial and ventricular myocytes, and was mediated only by L-type Ca^{2+} channels. The peak density of I_{Ca} was larger in ventricular cells than in atrial cells, and exceeded that reported for mammalian myocardium recorded under similar conditions. Steady-state SR Ca^{2+} content of quail myocardium was also larger than that reported for mammals, and reached $750.6 \pm 128.2 \mu\text{mol l}^{-1}$ in atrial cells and $423.3 \pm 47.2 \mu\text{mol l}^{-1}$ in ventricular cells at 24°C . We observed SR Ca^{2+} -dependent inactivation of I_{Ca} in ventricular myocytes, indicating cross-talk between sarcolemmal Ca^{2+} channels and ryanodine receptors in the SR. However, this phenomenon was not observed in atrial myocytes. Taken together, these findings help to explain the high-efficiency avian myocyte excitation–contraction coupling with regard to their reptilian-like cellular ultrastructure.

KEY WORDS: Bird, *Coturnix japonica*, Excitation–contraction coupling, Heart, L-type Ca^{2+} current, Sarcoplasmic reticulum

INTRODUCTION

Avian and mammalian hearts are morphologically similar in that they both possess four cardiac chambers: two atria and two ventricles. Their anatomically separated ventricular chambers are a key feature of endothermy as they allow systemic pressures to be substantially higher than pulmonary pressures, a pre-requisite for metabolically generated heat (Hicks and Wang, 2012; Jensen et al., 2013a,b). In contrast, the hearts of ectotherms generally exhibit

lower pressure development and differ in chamber number; fish have a two-chambered heart, and amphibians and reptilians for the most part possess three chambers. The evolution of the divided ventricle and separation of pulmonary and systemic pressures occurred at least twice, and independently in the bird and mammalian lineages (Hicks and Wang, 2012).

Despite gross morphological similarities, there are important differences between avian and mammalian hearts, which make birds particularly interesting with regard to vertebrate cardiac evolution. First, avian hearts are typically larger in relation to body mass than those of mammals and also have higher cardiac outputs, stroke volumes and arterial blood pressures (Grubb, 1983; Ruben, 1995). Second, this elevated cardiac performance is achieved with cardiomyocytes that superficially resemble those from reptiles more closely than those from mammals. Indeed, avian cardiomyocytes are long ($>100 \mu\text{m}$) and thin ($<10 \mu\text{m}$) and lack transverse (T)-tubules that are characteristic features of the myocytes which power the slower heart rates and lower contractile forces found in fish, amphibian and reptilian hearts (Dzialowski and Crossley, 2015; Shiels and Galli, 2014). Mammalian cardiomyocytes are shorter ($<100 \mu\text{m}$), thicker ($<30 \mu\text{m}$) and contain T-tubules (Richards et al., 2011) that are thought to be vital for the high maximal heart rates and robust contractility of mammalian hearts. Recent structural and computational modelling from Sheard et al. (2019) showed that the subcellular organization of Ca^{2+} release units (i.e. clusters of ryanodine receptors, RyRs) within the cardiac sarcoplasmic reticulum (SR) of birds could facilitate strong and fast contractions despite the long, thin, non-tubulated cellular ultrastructure. However, they did not support these findings with functional studies.

Both birds and mammals rely on Ca^{2+} release from the large intracellular SR network for cardiomyocyte contraction. This happens in response to trans-sarcolemmal Ca^{2+} entry through L-type calcium channels (LTCC). Extracellular Ca^{2+} influx (I_{Ca}) through LTCCs initiates the release of Ca^{2+} stored within the SR through RyRs in a process known as Ca^{2+} -induced Ca^{2+} release (CICR) (Fabiato, 1983). Close apposition (i.e. couplons) of LTCCs in the sarcolemma and RyRs in the SR membrane (Franzini-Armstrong et al., 2005) allow local control of Ca^{2+} release from the SR (Stern et al., 1997), fuelling the CICR process. In all adult mammalian ventricular myocytes studied to date (Forbes et al., 1990; Loughrey et al., 2004; Richards et al., 2011; Snelling et al., 2015), T-tubules bring the surface sarcolemma containing the LTCCs into close apposition with more centrally located SR membranes containing RyRs, ensuring simultaneous CICR within the entire volume of the thick mammalian cardiomyocyte (Franzini-Armstrong et al., 1999). Indeed, T-tubule abundance governs temporal and spatial properties of the ventricular Ca^{2+} transient in adult mammals and thus directly influences myocyte contraction (Dibb et al., 2013; Richards et al., 2011). In the more narrow piscine, reptilian and neonatal mammalian cardiomyocytes, and in atrial myocytes from small mammals, CICR occurs at peripheral couplings where the sarcolemma and the SR membranes juxtapose

¹Department of Human and Animal Physiology, Lomonosov Moscow State University, Leninskiye gory, 1, 12, Moscow 119234, Russia. ²Department of Physiology, Pirogov Russian National Research Medical University, Ostrovityanova str., 1, Moscow 117997, Russia. ³Ural Federal University, Mira 19, Ekaterinburg 620002, Russia. ⁴Laboratory of Cardiac Physiology, Institute of Physiology of Komi Science Centre of the Ural Branch of the Russian Academy of Sciences, FRC Komi SC UB RAS, Pervomayskaya str., 50, 167982 Syktyvkar, Komi Republic, Russia. ⁵Faculty of Biology, Medicine and Health, Core Technology Facility, 46 Grafton Street, University of Manchester, Manchester M13 9NT, UK.

*Author for correspondence (filatova@mail.bio.msu.ru)

 T.S.F., 0000-0003-0131-1911; D.V.A., 0000-0001-5751-8853

and then the Ca^{2+} signal diffuses centripetally to activate the interior of the narrow cell without the assistance of a T-tubular network (Bootman et al., 2006; Mackenzie et al., 2004; Shiels and Galli, 2014). A similar schema is proposed, but has not been measured, for avian cardiomyocytes where CICR at the periphery is coupled to specialized non-junctional SR known as corbular SR (Perni et al., 2012) which amplifies centripetal Ca^{2+} diffusion (Perni et al., 2012; Sheard et al., 2019).

There is a paucity of functional data on Ca^{2+} flux pathways in avian cardiomyocytes. Bogdanov et al. (1995) speculated that the high density of LTCC current together with the presence of T-type Ca^{2+} current in finch ventricular myocytes would drive strong CICR in the absence of T-tubules, but intracellular Ca^{2+} handling was not explored in this study. Thus, to improve our understanding of the relationship between structural organization of the myocyte and the strength and rate of cardiac contraction in Aves, the aim of this study was to (1) assess trans-sarcolemmal Ca^{2+} influx; (2) determine SR Ca^{2+} content and rate of refilling; and (3) to investigate cross-talk between LTCCs and RyRs in atrial and ventricular myocytes from the Japanese quail (*Coturnix japonica*). Our hypotheses were that (1) there would be large trans-sarcolemmal Ca^{2+} influx, which would mediate effective CICR from the SR; (2) SR Ca^{2+} content would be large and the SR would fill rapidly upon depletion; and (3) that there would be cross-talk between LTCC and RyRs in the bird heart, indicative of functional coupling (i.e. couplons) between sarcolemmal and SR membranes.

MATERIALS AND METHODS

Animals

Japanese quails (Estonian variety, *Coturnix japonica* Temminck and Schlegel 1849) of both sexes (age 2–4 months, weight 200–300 g, $N=15$) were obtained from a local farm (Orlovsky dvorik, Mytishchi, Moscow region, Russia). Although dilated cardiomyopathy, ascites and sudden death syndrome are not reported in meat-type Japanese quails, these complications are common for other domestic bird species (Jackson et al., 1972; Julian, 1987, 1998; Magwood and Bray, 1962; Nain et al., 2008). Thus, to avoid the risk of such diseases provoked by abnormally rapid growth, we chose a slow-growing egg-producing breed of quail for our study. Resting heart rates for these birds range between 318 ± 14 beats min^{-1} (Valance et al., 2008) and 531 ± 17 beats min^{-1} (Wilson, 1972) and mean arterial blood pressures are in the range of 125.75 ± 2.05 mmHg (Bavis and Kilgore, 2001) to 153.2 ± 4.5 mmHg (Ringer, 1968), confirming robust and rapid coordination of cellular Ca^{2+} fluxes and thus making them a suitable animal in which to address our hypotheses. The birds were kept at 24°C at 12 h:12 h photoperiod and fed with commercial quail food *ad libitum*. Birds were anesthetized with isoflurane (3.5% isoflurane and oxygen gas mixture supplied at a rate of 2 l min^{-1}), which is an effective anesthetic with minimal cardiovascular effects in birds (Naganobu and Hagio, 2000), and decapitated using a guillotine for small laboratory animals (OpenScience, Moscow, Russia). All experiments conform to the Guide for the Care and Use of Laboratory Animals published by the US National Institutes of Health (NIH Publication No. 85-23, revised 1996) and the EU Directive 2010/63/EU for animal experiments.

Cells isolation

We used the following protocol for enzymatic isolation of quail working (i.e. atrial and ventricular) cardiomyocytes (Abramochkin et al., 2017): following decapitation, the heart was quickly excised and mounted on a Langendorff apparatus for perfusion through the

middle branch of the aorta to perfuse the myocardium via the coronary arteries. The other two aortal branches were sealed with ligatures. The heart was perfused with nominally Ca^{2+} -free solution of the following composition (mmol l^{-1}): 116 NaCl, 4 KCl, 1.7 NaH_2PO_4 , 25 NaHCO_3 , 0.55 MgCl_2 , 5 sodium pyruvate, 20 taurine, 11 glucose, 1 g ml^{-1} bovine serum albumin; pH 7.4 maintained by aeration with carbogen (95% O_2 , 5% CO_2) at 42°C . After 7–9 min of perfusion and washing of blood from the heart, the perfusion was switched to the same solution supplied with 0.425 mg ml^{-1} collagenase II (Worthington Biochemical Corporation, Lakewood, NJ, USA), 0.025 mg ml^{-1} protease XIV (Sigma Aldrich, St Louis, MO, USA) and $6 \mu\text{mol ml}^{-1}$ CaCl_2 . After 30–39 min of enzymatic treatment the perfusion was stopped, and the atria and ventricles were separated and placed in Kraftbrühe solution (mmol l^{-1}): 3 MgSO_4 , 30 KCl, 30 KH_2PO_4 , 0.5 EGTA, 50 potassium glutamate, 20 Hepes, 20 taurine, 10 glucose; pH 7.2 adjusted with KOH (Isenberg and Klockner, 1982). Following digestion, atria were separated from the ventricles, placed into separate chambers and shaken to liberate myocytes. No attempt was made to separate the ventricles but due to chamber size, the majority of the ventricular cells isolated should be left-side in origin; however, we cannot exclude the possibility of some right-side ventricular cells being present in our recordings. Similarly, the atria were pooled together but the right is usually the larger of the two in birds (Dzialowski and Crossley, 2015) and although we did not quantify this, qualitatively we observed larger right atria in the Japanese quail and thus we anticipate a greater proportion of right atrial myocytes in this study. Atrial and ventricular cells were stored in Kraftbrühe solution at room temperature and used within 8 h after the isolation.

Recording of I_{Ca}

All ionic currents were recorded using perforated whole-cell patch clamp with a HEKA EPC-800 amplifier (HEKA Elektronik, Lambrecht, Germany). Isolated atrial or ventricular myocytes were placed into an experimental chamber (RC-26; Warner Instrument Corporation, Brunswick, CT, USA; volume $150 \mu\text{l}$) mounted onto an inverted microscope (Diaphot 200; Nikon, Tokyo, Japan). The cells were superfused with physiological solution of the following composition (mmol l^{-1}): 150 NaCl, 5.4 CsCl, 1.2 MgCl_2 , 5 Hepes, 2 CaCl_2 ; pH 7.4 adjusted with NaOH. Tetrodotoxin (TTX, $1 \mu\text{mol l}^{-1}$) was added to the solution to block fast sodium current (Marcus and Fozzard, 1981; Vornanen et al., 2011). The temperature of the extracellular solution in the experimental chamber was kept at 24°C (TC-324C; Warner Instrument Corporation). Patch pipettes were pulled from borosilicate glass capillaries without filament (Sutter Instruments, Novato, CA, USA) and filled with pipette solution. The pipette solution for I_{Ca} recordings contained (mmol l^{-1}): 130 CsCl, 1 MgCl_2 , 5 EGTA, 10 Hepes, 4 MgATP , 0.03 Na_2GTP , 15 tetraethylammonium; pH 7.2 adjusted with CsOH. This level of EGTA suppressed contractions and blocked outward Ca^{2+} -dependent currents (Vornanen, 1997). To study SR Ca^{2+} content we used a modified pipette solution containing (mmol l^{-1}): 130 CsCl, 5 MgCl_2 , 0.025 EGTA, 10 Hepes, 4 MgATP , 0.03 Na_2GTP , 15 tetraethylammonium; pH 7.2 adjusted with CsOH (Shiels et al., 2002). The lower concentration of EGTA in this solution was set to mimic physiological intracellular buffering (Creazzo et al., 2004; Hove-Madsen et al., 2001) and thus allowed effective and physiologically relevant cellular Ca^{2+} flux that was important for SR Ca^{2+} content assessment. All pipette solutions were provided with $40 \mu\text{mol l}^{-1}$ β -escin, a perforating ionophore, because it reduced rundown of calcium currents compared with the whole-cell configuration (not shown)

Table 1. SR Ca²⁺ content in atrial and ventricular cardiomyocytes of Japanese quail

No. of pulses	SR Ca ²⁺ content (μmol l ⁻¹)						
	5	10	15	25	50	75	100
Atria	119.2±21.1 [§]	185.5±25.9 [§]	337.4±67.3	474.8±138.5	530.2±139.5	638.5±170.3	750.6±128.2 [‡]
Ventricles	197.6±25.7	276.9±41.7 ^{**}	335.8±60.7 [*]	423.4±57.8	396±27.5	449.5±48.4	423.3±47.2 [‡]

Values are given as means±s.e.m. from 11–12 myocytes from 5–7 birds. Ca²⁺ concentration was calculated from the charge transferred in pC pF⁻¹ (see Fig. 3B) and with specific membrane capacity at 1.15 μF cm⁻², the surface:volume ratio for spindle-shaped cardiac cells at 1.15 and as a function of non-mitochondrial cytosolic volume at 55% (Creazzo et al., 2004; Vornanen, 1997; Vornanen et al., 1998). Steady-state SR Ca²⁺ content was reached after 15 pulses in atrial myocytes ([§]*P*<0.05 versus SR Ca²⁺ content at 15th pulse, repeated measures ANOVA) and by 25 pulses in ventricular myocytes (^{*}*P*<0.05, ^{**}*P*<0.01 versus SR Ca²⁺ content at 25th pulse, repeated measures ANOVA). [‡]Difference in SR Ca²⁺ content between atrial and ventricular myocytes (*P*<0.05, Student's *t*-test).

(Sarantopoulos et al., 2004). The resistance of filled patch pipettes was 2.3±0.4 MΩ. Access resistance and whole-cell capacitance were fully compensated after formation of the whole-cell configuration; mean access resistance was 3.9±0.6 MΩ at the time recordings began. The voltage-clamp protocols are shown in the corresponding figures.

To evaluate the interaction between trans-sarcolemmal Ca²⁺ influx via the LTCC (*I*_{Ca}) and intracellular Ca²⁺ release from the SR through RyRs, kinetics of *I*_{Ca} inactivation following SR Ca²⁺ release and progressive SR Ca²⁺ loading was recorded in atrial and ventricular myocytes. Previous studies show that intracellular Ca²⁺ (i.e. Ca²⁺ released from SR) enhances the inactivation of sarcolemmal *I*_{Ca} (Hadley and Lederer, 1991; Sham, 1997), and thus the dynamics of *I*_{Ca} inactivation can be used to estimate the interaction between these two Ca²⁺ sources (Shiels et al., 2002). We recorded *I*_{Ca} at 0 mV immediately after caffeine application and fitted a double exponential function (τ_f and τ_s) to its inactivating profile. The fitting was performed using the standard Chebyshev equation in Clampfit 10.3 software (Molecular Devices, San Jose, CA, USA).

Assessing SR Ca²⁺ content

We measured SR Ca²⁺ content by recording the inward current carried by Na⁺ ions pumped across the cell membrane by the Na⁺–Ca²⁺ exchanger (NCX) following the rapid application of caffeine. Caffeine causes SR RyRs to open, causing flow of Ca²⁺ from the SR to the cytosol down its concentration gradient. The released Ca²⁺ is then extruded from the cell by NCX in exchange for Na⁺ ions with stoichiometry of 1 Ca²⁺ to 3 Na⁺. In such conditions, NCX produces an inward current when membrane voltage (*V*_m) is held at –80 mV; the time integral of the NCX current (*I*_{NCX}) induced by caffeine is proportional to the amount of Ca²⁺ stored and released from SR at the time of application (Haverinen and Vornanen, 2009; Shiels et al., 2002; Varro et al., 1993). At the beginning of each experiment, rapid application of 10 mmol⁻¹ caffeine was used to empty the SR of Ca²⁺ whilst the *V*_m was held at –80 mV. The SR was then refilled by a series of square depolarizing pulses (from –80 to 0 mV, 200 ms, 1 Hz frequency). The capacity of the SR to reload

Ca²⁺ was estimated after 5, 10, 15, 25, 50, 75 and 100 pulses using rapid application (<1 s) of 10 mmol⁻¹ caffeine (Shiels et al., 2002). The obtained data were normalized by whole-cell capacitance and expressed as pC pF⁻¹. The SR Ca²⁺ content was also converted into a Ca²⁺ concentration in μmol l⁻¹ (Table 1) from the integral of *I*_{NCX} and the cell volume (Galli et al., 2011; Shiels et al., 2002). Cell volume was calculated from cell surface area [obtained by measurements of cell capacitance (pF) and assuming a specific membrane capacitance of 1.59 μF cm⁻²] and the surface:volume ratio of 1.15 (determined experimentally in previous studies of elongated cardiomyocytes; see Vornanen, 1997). Finally, SR Ca²⁺ content was expressed as a function of non-mitochondrial volume (55%), as determined previously (Creazzo et al., 2004; Vornanen et al., 1998).

Drugs

Collagenase type II was purchased from Worthington Biochemical Corporation. Protease type XIV, tetrodotoxin, nifedipine, caffeine and β-escin were purchased from Sigma.

Data analysis and statistics

All data are presented as means±s.e.m. from *n* cells. The number of cells tested is indicated in figure legends together with number of birds (*N*). The amplitude of currents and the charge transferred by *I*_{NCX} were normalized by cell capacitance. Student's *t*-test was used to compare current densities and SR Ca²⁺ content in atrial and ventricular cardiomyocytes. One-way repeated measures analysis of variances (ANOVA) followed by Dunnett's *post hoc* test was used to separately evaluate the effect of pulse number on Ca²⁺ accumulation in SR and on the inactivation kinetics of *I*_{Ca}. The differences were considered statistically significant at *P*<0.05.

RESULTS

Morphology of quail cardiomyocytes

Retrograde enzymatic perfusion of quail hearts yielded a large number of thin, long, spindle-shaped cells with clear cross-striation. Ventricular myocytes (Fig. 1A) were on average 179.3±13.9 μm in length and 8.32±0.43 μm wide (*n*=13, *N*=3), whilst atrial myocytes (Fig. 1B) were significantly smaller: 130.6±5.32 μm in length and

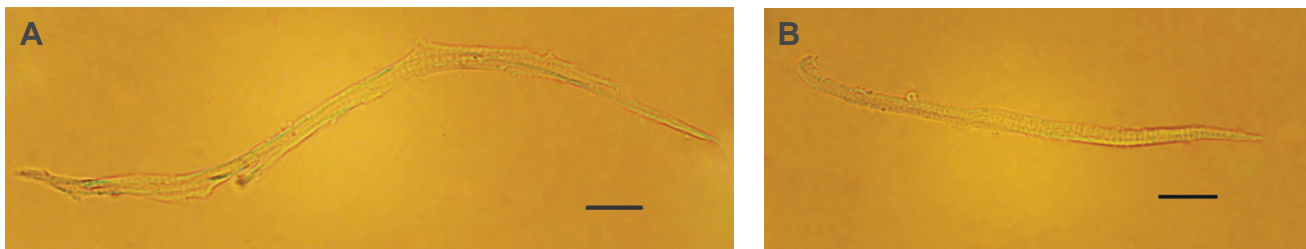


Fig. 1. Morphology of quail cardiomyocytes. Photomicrographs of enzymatically isolated quail ventricular (A) and atrial (B) cardiomyocytes. Morphometric measurements are described within the text. Scale bars, 20 μm.

$6.78 \pm 0.47 \mu\text{m}$ wide ($n=13$, $N=3$; $P < 0.01$ for length, $P < 0.05$ for width; Student's *t*-test). These differences in linear dimensions were reflected in cell capacitance, which is an index of cell surface area: 55.82 ± 1.91 pF for ventricular cells ($n=35$, $N=7$) and 38.65 ± 1.52 pF for atrial cells ($n=37$, $N=7$) ($P < 0.0001$, Student's *t*-test).

Sarcolemmal I_{Ca} in isolated quail cardiomyocytes

Sarcolemmal Ca^{2+} current (Fig. 2A,B) was elicited in isolated quail cardiomyocytes using a square-pulse protocol (Fig. 2C) from the holding potential (V_h) of -90 mV in the presence of $1 \mu\text{mol l}^{-1}$ TTX to block I_{Na} . Preliminary data (not shown) supports earlier findings that I_{Na} in avian myocytes is TTX sensitive, thus allowing Ca^{2+} influx to be measured from a physiological V_h (Marcus and Fozzard, 1981; Vormanen et al., 2011). Fig. 2 shows the representative recordings of I_{Ca} in atrial (Fig. 2A) and ventricular (Fig. 2B) myocytes and its current–voltage relations (Fig. 2C) at room temperature (24°C). I_{Ca} activated at potentials positive to -40 mV. The maximum peak current was observed at 0 mV and in ventricular cells it was significantly greater than in atrial myocytes. It is noteworthy that the peak amplitude of I_{Ca} in ventricular cells was remarkably high (-10.2 ± 1.15 pA pF $^{-1}$) in comparison with I_{Ca} recorded in mammalian cardiomyocytes in similar conditions (Mitrokhin et al., 2019; Ogura et al., 1999) indicating robust

trans-sarcolemmal influx in the ventricular cells. In line with findings in embryonic chicken myocytes (Kitchens et al., 2003), we found that $50 \mu\text{mol l}^{-1}$ nifedipine completely abolished I_{Ca} in both atrial and ventricular cells from quail (not shown).

The lack of an inward current at potentials negative to -40 mV suggests the absence of the T-type Ca^{2+} current (I_{CaT}) (Xu and Best, 1992) in quail cardiomyocytes (Fig. 2C). However, as prominent I_{CaT} has been recorded in cardiomyocytes of finch (Bogdanov et al., 1995) and embryonic chicken (Brotto and Creazzo, 1996; Creazzo et al., 2004; Kitchens et al., 2003), we wanted to probe this more thoroughly. We therefore elicited I_{Ca} with a modified square-pulse protocol from the V_h of -50 mV (see Fig. 2D), which should inactivate any potential I_{CaT} and allowed us to record I_{CaL} only. Indeed, the component activated by square pulses from $V_h = -90$ mV and inactivated at $V_h = -50$ mV has been referred to as I_{CaT} (Haworth et al., 2014). The corresponding current–voltage relationship for I_{Ca} in atrial and ventricular myocytes (Fig. 2D) shows that the Ca^{2+} current elicited by both protocols activates at -40 mV and has maximum amplitude at 0 mV, which is characteristic of I_{CaL} . Together with complete inhibition of the current with $50 \mu\text{mol l}^{-1}$ nifedipine (not shown), we confirm that I_{CaT} is not present in cardiomyocytes from the adult quail, and I_{Ca} consists entirely of I_{CaL} .

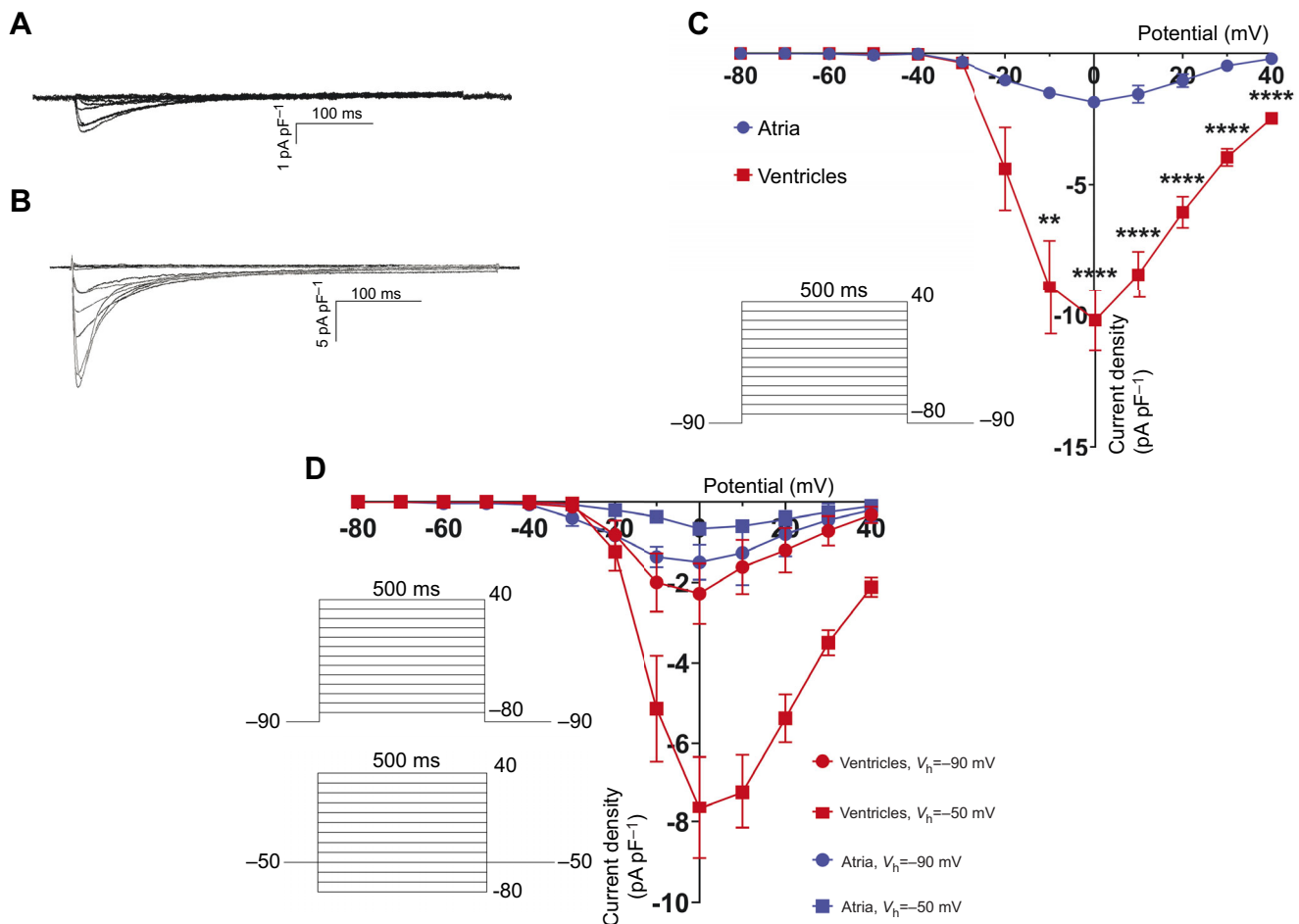


Fig. 2. Characteristics of I_{Ca} in quail cardiomyocytes. Representative recordings of I_{Ca} in atrial (A) and ventricular (B) cardiomyocytes. The voltage-clamp protocols used to record the currents in A and B are shown in the inset of C. (C) Current–voltage relationship of I_{Ca} recorded in atrial ($n=7$, $N=3$) and ventricular ($n=8$, $N=3$) quail cardiomyocytes (** $P < 0.01$, **** $P < 0.0001$, Student's *t*-test). (D) Current–voltage relationships of the differential I_{Ca} elicited from the holding potentials (V_h) of -90 mV (round symbols) and -50 mV (square symbols) in atrial ($n=6$, $N=3$) and ventricular ($n=7$, $N=3$) cardiomyocytes. The peak at 0 mV and the absence of current at potentials more negative than -40 mV indicate that I_{CaT} is absent in quail working myocardium.

Sarcoplasmic reticulum Ca^{2+} content

At the beginning of each experiment, we applied 10 mmol^{-1} caffeine to empty the SR Ca^{2+} stores, such that each experiment began with the cell in the same state (see Shiels et al., 2002). After depletion of SR Ca^{2+} stores, we applied 5–100 square depolarizing pulses (from -80 to 0 mV , 200 ms) at a frequency of 1 Hz to load the SR with Ca^{2+} and assess progressive SR Ca^{2+} loading using rapid caffeine application. At V_h of -80 mV , caffeine-induced Ca^{2+} release from SR activated NCX, which pumped the excess of Ca^{2+} from the cytoplasm and therefore produced an inward current (I_{NCX}). I_{NCX} was measured in voltage-clamp mode (Fig. 3A) and time integral of this current was used to calculate SR Ca^{2+} content in pC pF^{-1} (Fig. 3B).

All cells accumulated SR Ca^{2+} during the depolarizing pulses. In ventricular cardiomyocytes SR Ca^{2+} content reached a steady-state level after 25 pulses (i.e. after 25 pulses there were no statistically significant changes in SR content with further depolarizing pulses). In atrial cells, steady-state Ca^{2+} content was reached after 15 pulses (Fig. 3B). SR Ca^{2+} content in atrial myocytes was higher than in ventricular cells, and reached statistical significance at 100 pulses where SR Ca^{2+} content was $1.23 \pm 0.14 \text{ pC pF}^{-1}$ in ventricular myocytes and $2.19 \pm 0.37 \text{ pC pF}^{-1}$ in atrial myocytes. The SR Ca^{2+} content at each stage of SR Ca^{2+} loading for each cell type was converted from pC pF^{-1} to Ca^{2+} concentration in $\mu\text{mol l}^{-1}$ (Table 1) from the integral of I_{NCX} and the cell volume.

Interaction between sarcolemmal I_{Ca} and SR Ca^{2+} release

Trans-sarcolemmal Ca^{2+} influx through LTCCs triggers the release of Ca^{2+} stored within the SR through RyRs in a process termed CICR. However, because the inactivation of I_{Ca} is both voltage and Ca^{2+} dependent, Ca^{2+} released from the SR can also feed back and affect sarcolemmal Ca^{2+} influx. To investigate this interaction in the quail heart, I_{Ca} elicited with square depolarizing pulses was recorded immediately following the depletion of SR Ca^{2+} stores by caffeine and during the series of pulses that reloaded SR Ca^{2+}

stores (Fig. 4A). The influence of SR Ca^{2+} accumulation (and thus potential SR Ca^{2+} release) on trans-sarcolemmal influx was estimated by changes in inactivation kinetics of I_{Ca} . The current traces in Fig. 4A illustrate the change in the inactivation kinetics of ventricular I_{Ca} when the SR is empty and thus unable to release Ca^{2+} in response to trans-sarcolemmal influx (i.e. pulse 1) and when the SR contains Ca^{2+} that is available for CICR (i.e. pulses 2–10). The cross-talk between Ca^{2+} released from the SR and the LTCC is quantified by the inactivation time constants of I_{Ca} which were best fit with double exponential functions representing the fast (τ_f ; Fig. 4C) and slow (τ_s ; Fig. 4D) component of inactivation, respectively (also see Table 2). Fig. 4C,D shows progressively faster inactivation kinetics for ventricular myocytes as the SR is filled with Ca^{2+} by the loading pulses, indicative of cross-talk between the two Ca^{2+} flux systems. Furthermore, because the amplitude of I_{Ca} did not change during consecutive loading pulses (Fig. 4A), the change in inactivation kinetics (Fig. 4C,D) observed with progressive SR Ca^{2+} loading is unlikely to result from voltage-dependent inactivation or Ca^{2+} -dependent inactivation from Ca^{2+} entry through the LTCC itself. Surprisingly, despite the high maximal SR Ca^{2+} content in atrial myocytes (Table 1), we did not find evidence of cross-talk between the SR and LTCCs in atrial myocytes (Fig. 4B–D; Table 2).

DISCUSSION

The present study is the first to describe SR Ca^{2+} content in an adult avian heart, and the second (Bogdanov et al., 1995) to study ionic currents in isolated adult cardiomyocytes. Bird cardiomyocytes differ from mammalian cardiomyocytes in terms of morphology and ultrastructure, and due to their spindle shape and the absence of T-tubules, more closely resemble cardiomyocytes of ectothermic vertebrates (reptilians, amphibians, fish) than mammals (Dzialowski and Crossley, 2015; Shiels and Galli, 2014). However, unlike ectotherms, bird hearts contract at high rates and with more force, providing circulatory convection sufficient to

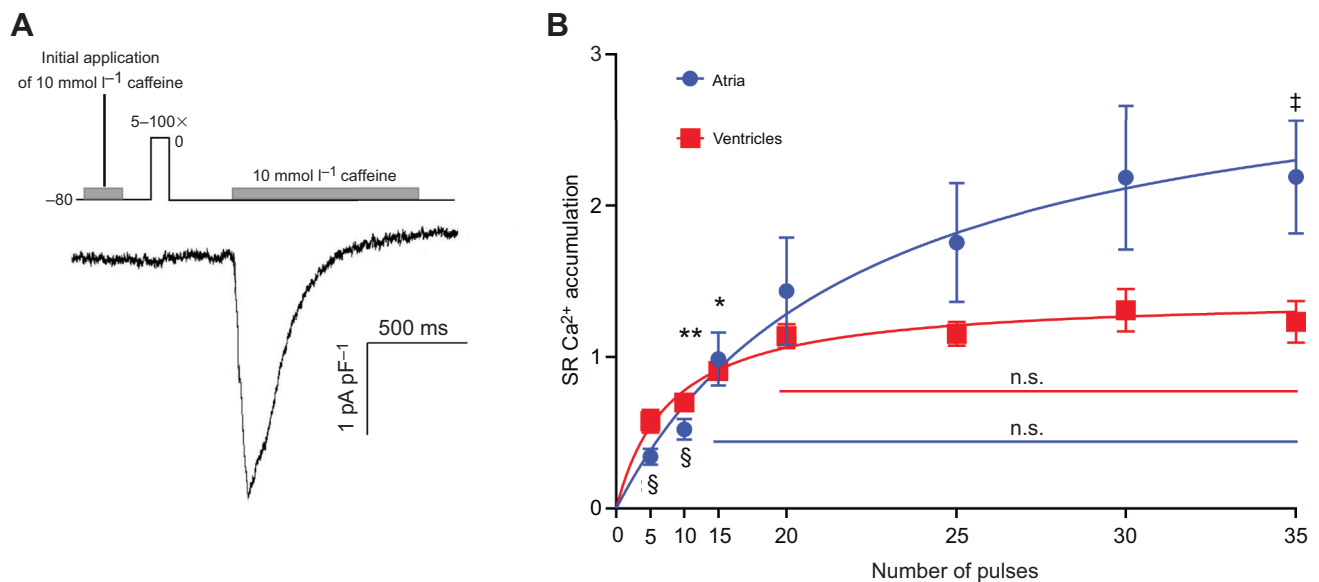


Fig. 3. Steady-state SR Ca^{2+} content in quail working myocardium. (A) Schema of the experiment (top) and a representative recording of I_{NCX} induced by rapid application of caffeine in an atrial myocyte. (B) SR Ca^{2+} accumulation expressed as the charge transfer (pC) normalized to cell size (pF) in atrial (blue symbols, $n=11$, $N=6$) and ventricular (red symbols, $n=13$, $N=5$) quail cardiomyocytes ($^{\dagger}P<0.05$, Student's t -test). Steady-state SR Ca^{2+} content was reached after 15 pulses in atrial myocytes ($^{\S}P<0.05$ versus SR Ca^{2+} content at 15th pulse, repeated measures ANOVA) and by 25 pulses in ventricular myocytes ($^*P<0.05$, $^{**}P<0.01$ versus SR Ca^{2+} content at 25th pulse, repeated measures ANOVA; n.s., not significant).

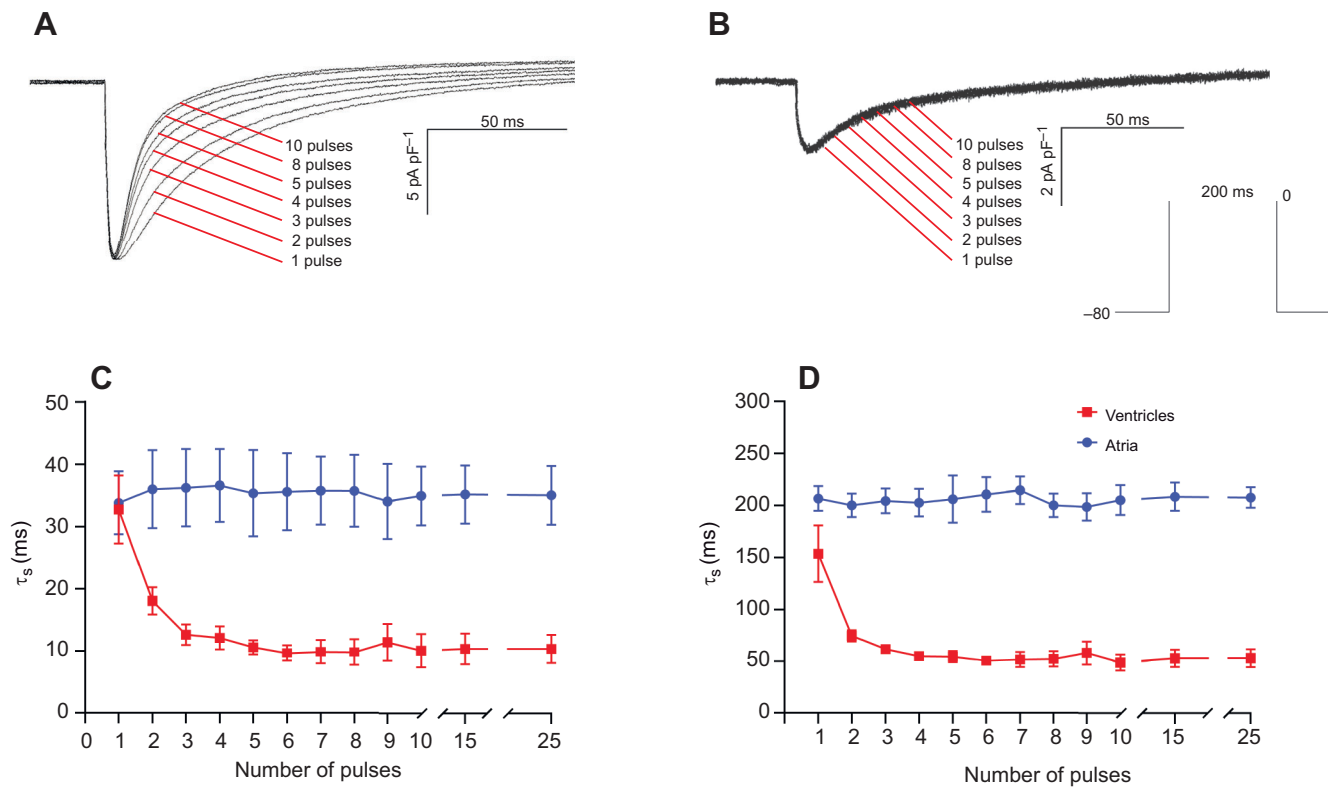


Fig. 4. The effect of SR Ca^{2+} accumulation on inactivation kinetics of sarcolemmal I_{Ca} in quail cardiomyocytes. Representative recordings of I_{Ca} in an isolated quail ventricular (A) and atrial (B) myocyte stimulated with square depolarizing pulses (voltage-clamp protocol shown in the inset) immediately after the depletion of SR Ca^{2+} store with caffeine (pulse 1) and SR refills with additional pulses (pulses 2–10). (C,D) Inactivation time constants (τ_f and τ_s , respectively) of I_{Ca} in ventricular and atrial quail cardiomyocytes during the course of SR Ca^{2+} refilling following caffeine application. τ_f and τ_s were obtained from double exponential fitting of the inactivating part of I_{Ca} (* $P < 0.05$, Student's paired t -test, $n = 7$, $N = 3$).

maintain endothermic energy metabolism. Our previous work (Sheard et al., 2019) and that of others (Bogdanov et al., 1995; Brotto and Creazzo, 1996; Kim et al., 2000; Pemi et al., 2012; Tanaka et al., 1995) suggested efficient CICR, coupled with specialized structural organization of the avian SR, could facilitate 'mammalian-like' contractility in 'reptilian-like' myocytes. This led us to hypothesize that in quail cardiomyocytes there would be: (1) a large trans-sarcolemmal Ca^{2+} influx, which would mediate effective CICR; (2) a large SR Ca^{2+} content that would fill rapidly upon depletion; and (3) that there would be cross-talk between LTCC and RyRs in the bird heart indicative of functional coupling between sarcolemmal and SR membranes. Our data allow us to accept each of these hypotheses for ventricular myocytes providing the functional evidence to support structural and functional

coordination of CICR as a means to deliver strong and fast contractions in the quail ventricle. However, in comparison with the ventricle, quail atrial myocytes exhibited smaller trans-sarcolemmal Ca^{2+} influx, larger maximal SR Ca^{2+} content, and showed no evidence of cross-talk between LTCCs and RyRs. Thus, our study reinforces the connection between structural organization of the myocyte and the strength and rate of cardiac contraction across vertebrate classes, whilst highlighting key atrioventricular differences.

Cellular morphology

The similarity in gross cellular morphology between bird and reptile myocardium has been known via electron microscopy for more than 50 years (Hirakow, 1970). Fig. 1 shows the gross cellular morphology for freshly isolated intact cardiomyocytes from the quail, which are similar to those reported for ectothermic vertebrates including fish (crucian carp and scombrids, Vornanen, 1997; Shiels et al., 2004), reptiles (turtle, Galli et al., 2006; lizard, Galli et al., 2009) and other birds (turkey, Kim et al., 2000; chicken, Akester, 1981; finch, Bogdanov et al., 1995; finch, Bossen et al., 1978). Moreover, like other vertebrate species (reviewed in Shiels and Galli, 2014), quail atrial cells are smaller than ventricular cells (Fig. 1). The narrow width of the quail myocytes means that, even in the absence of T-tubules, Ca^{2+} release via peripheral couplings at the surface sarcolemma does not have far to travel to release more centrally located SR Ca^{2+} stores. Because T-tubules improve temporal and spatial properties of the Ca^{2+} transient and thus contraction, tubulated myocytes are often considered to have more robust cellular Ca^{2+} cycling (i.e. a faster rate of rise and larger

Table 2. The effect of SR Ca^{2+} ($\mu\text{mol l}^{-1}$) content on the inactivation kinetics of I_{Ca} in isolated atrial and ventricular cardiomyocytes of Japanese quail

	τ_f		τ_s	
	SR empty	SR full	SR empty	SR full
Atria	33.81 \pm 5.05	34.88 \pm 4.72	206.8 \pm 11.84	205.2 \pm 14.36
Ventricles	32.75 \pm 5.45	10.05 \pm 2.65*	153.6 \pm 27.2	48.87 \pm 7.52*

Values are given as means \pm s.e.m. from 6–7 myocytes per tissue type from a minimum of three birds. τ_f , fast time constant of I_{Ca} inactivation; τ_s , slow time constant of I_{Ca} inactivation. I_{Ca} was elicited with square pulses (from -80 to 0 mV, 200 ms), and the inactivation of I_{Ca} was fitted with a double exponential function. *Statistically significant differences between time constants with empty and steady-state Ca^{2+} -loaded SR ($P < 0.05$, Student's paired t -test).

systolic Ca^{2+} transient and thus contraction) than narrow cardiomyocytes. This makes the pairing of narrow myocytes and powerful pumping capacity in the avian heart particularly interesting. Notably, cardiomyocyte width appears to be the factor determining the presence or absence of a T-tubular system in the vertebrate heart. Ventricular myocytes from adult mammals (independent of heart size) are on average $>25\ \mu\text{m}$ in width (e.g. mouse, rat, rabbit, horse; Loughrey et al., 2004) and it is now accepted that atrial myocytes from large mammals (e.g. sheep, cow, horse and human) also contain T-tubules and that T-tubular abundance correlates with atrial myocyte width (Bootman et al., 2006; Mackenzie et al., 2004; Richards et al., 2011). It is interesting to note that mammalian myocytes are devoid of T-tubules and have limited SR function, but both develop during ontogeny, coincident with an increase in myocyte width (Shiels and Galli, 2014).

Trans-sarcolemmal Ca^{2+} influx

The sarcolemmal Ca^{2+} current registered in quail cardiomyocytes had conventional current–voltage configurations and the observed difference in current density between atrial and ventricular myocytes is a common phenomenon for vertebrate hearts (Badr et al., 2018; Filatova et al., 2019; Hatano et al., 2006). Of note is the large amplitude of I_{Ca} in quail ventricular myocytes. This correlates with a comparative study between finch and rat ventricular myocytes where the peak current density of I_{Ca} in the avian cells exceeded that of the rodent cells by 52% (Bogdanov et al., 1995). Fabiato (1983, 1985) revealed that the greater the magnitude of I_{Ca} , the greater the trigger for SR Ca^{2+} release. Thus the gain of CICR (e.g. the amount of Ca^{2+} released from the SR as a function of the trans-sarcolemmal Ca^{2+} trigger) may be particularly high in bird myocytes to power their strong and fast contractions (as discussed further below).

The large I_{Ca} current density reported here for quail ventricular cells is greater than that of ectotherms (i.e. roach, Badr et al., 2018; turtle, Galli et al., 2006; lizard, Galli et al., 2009; sturgeon, Haworth et al., 2014; rainbow trout, Vornanen et al., 1998) who do not utilize SR Ca^{2+} stores during excitation–contraction coupling (Shiels and Galli, 2014; Shiels and Sitsapesan, 2015). However, and interestingly, fish of the scombrid family (tunas, mackerel), who are renowned for their high level of activity, high metabolic rate, and for routine utilization of SR Ca^{2+} stores during excitation–contraction coupling, also exhibit large I_{Ca} peak current densities. In a series of experiments performed under the same conditions as the present study (i.e. at room temperature with $5\ \text{mmol l}^{-1}$ EGTA in the pipette solution), pacific mackerel *Scomber japonicus* (Shiels et al., 2004), yellowfin tuna *Thunnus albacares* and bluefin tuna *Thunnus orientalis* ventricular myocytes demonstrated comparatively high I_{Ca} density and SR Ca^{2+} content (Galli et al., 2011). Thus, the robust trans-sarcolemmal I_{Ca} reported here for quail supports our first hypothesis and idea that a large-amplitude I_{Ca} may be a feature of cardiomyocytes that rely on CICR, particularly in species that lack T-tubules. Interestingly, this pattern might be not true for highly active non-vertebrate species, such as cephalopods, where cardiomyocytes from the systemic heart displayed large SR Ca^{2+} stores and a large SR contribution to cardiac contractility but were associated with rather small trans-sarcolemmal Ca^{2+} currents (Altimiras et al., 1999).

It is important to consider the impact of temperature on I_{Ca} . At *in vivo* body temperatures of approximately $37\text{--}39^\circ\text{C}$, peak I_{Ca} is expected to be even greater in birds than that reported here from room temperature studies. The corollary is that comparable I_{Ca} current densities reported above for scombrid fishes would be

reduced at *in vivo* temperatures. Indeed, the Q_{10} for peak I_{Ca} amplitude is around 2 across a range of vertebrates [e.g. Q_{10} is: ~ 2 for rainbow trout (Shiels et al., 2000); ~ 1.8 for guinea pig and ground squirrel ventricle (Herve et al., 1992); ~ 2.9 for guinea-pig ventricle (Cavalié et al., 1985); and ~ 2.7 for rabbit ventricle (Shimoni and Banno, 1993)]. As the amplitude of I_{Ca} is important for the gain of SR Ca^{2+} release (Fabiato, 1983), strong CICR is expected for both chambers of the avian heart at *in vivo* body temperatures.

There are very few electrophysiological studies on trans-sarcolemmal Ca^{2+} influx in avian myocardium, with some reporting the presence (adult finch, Bogdanov et al., 1995; embryonic chicken, Brotto and Creazzo, 1996; Creazzo et al., 2004; Kitchens et al., 2003) and others reporting the absence (adult turkey, Kim et al., 2000) of T-type Ca^{2+} (I_{CaT}) influx. In finch ventricular myocytes, I_{CaT} had significant amplitude (60% of I_{CaL} amplitude) which is atypical for working myocardium of adult mammals (Bogdanov et al., 1995). As T-type Ca^{2+} currents are often present in neonatal mammalian myocytes (Xu and Best, 1992), it has been hypothesized that they are important for excitation–contraction coupling in cardiomyocytes lacking T-tubules and in cell types where the SR is under-developed. This is supported by data from chicken embryos where a prominent I_{CaT} current is recorded but which decreases over the course of embryonic development concurrent with the development of the SR and an increase in its Ca^{2+} content (Creazzo et al., 2004; Kawano and DeHaan, 1991; Kitchens et al., 2003). Nevertheless, from the electrophysiological data obtained in the current study, we can conclude that I_{Ca} in quail myocardium consists only of L-type Ca^{2+} current (I_{CaL}), presumably from $\text{Ca}_v1.2$ and $\text{Ca}_v1.3$ channel isoforms, according to the configuration of the current–voltage curve (Park et al., 2015).

SR Ca^{2+} content

Contractile force production in avian hearts is known to rely heavily on Ca^{2+} release from the SR. Indeed, Tanaka et al. (1995) used isolated trabecular muscle preparations from newly hatched chicken hearts to show that more than 50% of the Ca^{2+} required for contraction came from the SR. Similarly, Creazzo et al. (2004) showed $>50\%$ reductions in the intracellular Ca^{2+} transient following SR inhibition in late-stage embryonic chicken myocytes. Additionally, SR vesicles from adult turkey ventricular homogenates demonstrated robust SERCA activity (Gwathmey et al., 1999). These functional studies indicating robust intracellular Ca^{2+} cycling are coupled with decades of ultrastructural investigations showing specialized SR, including corbular SR, and extended junctional SR (a special form of junctional SR) containing RyRs clustered along Z-lines in avian heart (Junker et al., 1994; Pemi et al., 2012; Sheard et al., 2019; Sommer and Jennings, 1986). Together these features clearly indicate that both intracellular and extracellular Ca^{2+} cycling pathways underlie the powerful output of avian hearts. However, there exists only a single study where SR Ca^{2+} has been assessed in birds (embryonic chicken myocytes; Creazzo et al., 2004) and no studies we are aware of which probe the functional coupling between extra- and intracellular Ca^{2+} flux systems in birds.

Here we report a large steady-state SR Ca^{2+} content in adult myocytes of quail that refills rapidly after emptying by caffeine (Fig. 3; Table 1). This finding allows us to accept the second hypothesis of this study for both atrial and ventricular myocytes. After 15 loading pulses SR Ca^{2+} content begins to stabilize and at 25 pulses it reaches $\sim 425\ \mu\text{mol l}^{-1}\ \text{Ca}^{2+}$ in both atrial and ventricular

cells (Table 1) which compares favourably with the SR Ca^{2+} content reported for late stage embryonic chicken myocytes ($\sim 400 \mu\text{mol l}^{-1} \text{Ca}^{2+}$; Creazzo et al., 2004). The larger SR Ca^{2+} content (after 100 pulses; Table 1) in quail atrial cells compared with ventricular cells is consistent with atrioventricular differences in SR Ca^{2+} storage capacities reported for other vertebrates (burbot, trout and carp, Haverinen and Vornanen, 2009; rat, Walden et al., 2009). Although direct comparisons are difficult due to different Ca^{2+} loading protocols between the studies, in general steady-state content is reached between 15 and 25 pulses in the quail heart, which is faster than that described for ectotherms (>25 pulses, Haverinen and Vornanen, 2009; Shiels et al., 2002), but slower than mammals (5–10 pulses, Delbridge et al., 1996; Ginsburg et al., 1998).

The steady-state SR Ca^{2+} content in quail myocytes is comparable to that reported for a number of fish species (including rainbow trout, carp, mackerel and tuna; Haverinen and Vornanen, 2009; Shiels and Galli, 2014) and greatly exceeds those reported for mammals ($50\text{--}200 \mu\text{mol l}^{-1} \text{Ca}^{2+}$) when both are assessed by the application of 10 mmol l^{-1} caffeine (Negretti et al., 1995; Venetucci et al., 2006). In fishes, the limited SR Ca^{2+} release during excitation–contraction coupling relative to the high Ca^{2+} storage capacity of the SR has been explained in part by the low density of RyRs, their organization into calcium release units (CRUs), the proximity of CRUs to LTCCs (i.e. formation of couplons) and SR regulation (e.g. RyR sensitivity to opening from both cytosolic and luminal sides) (see Shiels and Sitsapesan, 2015). The lower steady-state SR Ca^{2+} content in mammals can also be explained by the subcellular organization of CRUs and regulation of RyRs, which results in spontaneous release of SR Ca^{2+} and the formation of Ca^{2+} waves when the SR Ca^{2+} content exceeds a threshold of $60\text{--}100 \mu\text{mol l}^{-1} \text{Ca}^{2+}$, depending on conditions (Venetucci et al., 2006). The finding of large SR Ca^{2+} stores and significant reliance on CICR for excitation–contraction coupling in the quail heart is intriguing and adds to our awareness of the fundamental differences between the way in which luminal Ca^{2+} controls RyR opening in ectotherms, birds and mammals. Although we know little about Ca^{2+} buffering in bird heart, Creazzo et al. (2004) demonstrated a lower cytosolic Ca^{2+} buffering capacity in embryonic birds than that observed for mammals, thus the low level of cytosolic buffering achieved via inclusion of EGTA ($25 \mu\text{mol l}^{-1}$) in the pipette solution during assessment of SR Ca^{2+} content and CICR is unlikely to account for the large SR Ca^{2+} content observed. Moreover, $[\text{H}^3]$ ryanodine binding studies in pigeon and finch heart show that the density of RyRs and the cytosolic Ca^{2+} sensitivity of RyRs in birds are generally similar to mammals (Junker et al., 1994). Interestingly, Creazzo et al. (2004) also observed an increase in SR Ca^{2+} buffering capacity during embryonic development in chicken myocytes, which coincided with an increase in the per cent SR involvement in excitation–contraction coupling and in the gain of CICR. Thus, future work should examine the Ca^{2+} buffering capacity of the adult bird SR and the sensitivity of RyR opening to both luminal and cytosolic Ca^{2+} as well as other regulators of SR function at *in vivo* body temperatures.

Cross-talk between sarcolemmal and SR Ca^{2+} fluxes

The third hypothesis of this study is that there would be cross-talk between LTCC and RyRs in the bird heart, indicative of functional coupling between sarcolemmal and SR membranes. More than two decades of structural studies on avian myocardium have demonstrated apposition of the two membrane systems and the presence of RyRs in the intermembrane space (Akester, 1981; Bossen et al., 1978; Hirakow, 1970; Junker et al., 1994; Pemi et al., 2012). However, to

our knowledge, no avian study has quantified this interaction functionally. Our finding of SR Ca^{2+} content-dependent changes in the inactivation kinetics of I_{Ca} in quail ventricular myocytes confirms LTCC and RyRs cross-talk (Fig. 4; Table 2) and thus allows us to accept the third hypothesis for ventricular myocardium.

The lack of a similar interaction in atrial myocytes may be due to less favourable ultrastructural organization in atrial tissue compared with ventricular tissue, and/or to the reduced amplitude of I_{Ca} registered in atrial myocytes which would reduce the gain of CICR. Indeed, studies with rainbow trout have shown that CICR and LTCC–RyR cross-talk can be amplified by adrenergic stimulation directly increasing the amplitude of I_{Ca} (Cros et al., 2014). Indeed, Cros et al. (2014) suggest the I_{Ca} trigger must be $>6 \text{ pA pF}^{-1}$ for CICR in trout heart. It is important to note that at *in vivo* body temperatures, quail atrial I_{Ca} may be of sufficient magnitude to trigger SR Ca^{2+} release and thus future work should be conducted at $\sim 38^\circ\text{C}$ to establish the I_{Ca} threshold for avian atrial CICR. The inability to trigger SR Ca^{2+} release in the atrial cells may underlie their higher SR Ca^{2+} content and implies that atrial RyRs (like those of fish cardiomyocytes; Shiels and Sitsapesan, 2015) do not open spontaneously at high luminal Ca^{2+} content. Nothing is known about how cytosolic or luminal ligands and proteins interact with avian RyRs, so research in this area would be extremely informative.

The degree of SR Ca^{2+} -dependent accelerated inactivation of I_{Ca} reported here for quail ventricular myocytes (Table 2) again highlights the strong gain of CICR in the bird heart. Unfortunately, direct comparison of avian and other vertebrate data is difficult due to different loading protocols. Nevertheless, in studies at room temperature, in mammalian cells acceleration of I_{Ca} inactivation reached steady state in 5 pulses after caffeine application (Adachi-Akahane et al., 1996; Sham, 1997) compared with ~ 5 in quail (Fig. 4C,D; Table 2) and ~ 20 in fishes (Shiels et al., 2002). Separating out the contribution of I_{Ca} and RyR clustering/regulation in achieving this robust coupling between the sarcolemmal trigger and the SR Ca^{2+} release in the bird heart would extend the findings presented here and shed important light on the evolution of these Ca^{2+} cycling pathways in vertebrate hearts.

Perspectives on avian excitation–contraction coupling

Despite gross morphological similarities, there are important differences between bird and mammalian hearts, which make birds particularly interesting with regard to cardiac evolution. The seeming paradox of ‘reptilian-like’ cardiomyocyte powering a metabolism capable of supporting flight has fascinated zoologists and cardiologists across the ages and driven research across multiple levels of biological, ontogenetic and phylogenetic organization (Altimiras et al., 2017; Boukens et al., 2019; Hillman and Hedrick, 2015; Hirakow, 1970; Shiels and Galli, 2014). In this paper, we attempt to functionally test hypotheses linking cellular SR ultrastructure with excitation–contraction coupling in the avian heart. Our findings of strong trans-sarcolemmal Ca^{2+} influx and a high gain of CICR, support these earlier suggestions that the organization of CRUs and the short diffusional distance for Ca^{2+} transport in the narrow cells allows for strong and fast contractions in avian myocytes. Thus, our study reinforces the connection between structural organization of the myocyte and the strength and rate of cardiac contraction across vertebrate classes. The findings also raise important questions about the regulation of Ca^{2+} release from the SR in birds. As many human cardiomyopathies are associated with errant SR Ca^{2+} release, understanding how bird hearts regulate their luminal Ca^{2+} release could have interesting therapeutic implications.

Competing interests

The authors declare no competing or financial interests.

Author contributions

Conceptualization: H.A.S.; Methodology: H.A.S.; Formal analysis: T.S.F.; Investigation: T.S.F.; Resources: D.V.A.; Data curation: T.S.F.; Writing - original draft: T.S.F., H.A.S.; Writing - review & editing: T.S.F., D.V.A., H.A.S.; Visualization: T.S.F.; Supervision: H.A.S.; Project administration: D.V.A.; Funding acquisition: D.V.A.

Funding

The study was supported by the Russian Foundation for Basic Research (19-34-90142 to D.V.A.).

References

- Abramochkin, D. V., Karimova, V. M., Filatova, T. S. and Kamkin, A.** (2017). Diadenosine pentaphosphate affects electrical activity in guinea pig atrium via activation of potassium acetylcholine-dependent inward rectifier. *J. Physiol. Sci.* **67**, 523-529. doi:10.1007/s12576-016-0510-z
- Adachi-Akahane, S., Cleemann, L. and Morad, M.** (1996). Cross-signaling between L-type Ca^{2+} channels and ryanodine receptors in rat ventricular myocytes. *J. Gen. Physiol.* **108**, 435-454. doi:10.1085/jgp.108.5.435
- Akester, A. R.** (1981). Intercalated discs, nexuses, sarcoplasmic reticulum and transitional cells in the heart of the adult domestic fowl (*Gallus gallus domesticus*). *J. Anat.* **133**, 161-179.
- Altimiras, J., Hove-Madsen, L. and Gesser, H.** (1999). Ca^{2+} uptake in the sarcoplasmic reticulum from the systemic heart of octopod cephalopods. *J. Exp. Biol.* **202**, 2531-2537.
- Altimiras, J., Lindgren, I., Giraldo-Deck, L. M., Matthei, A. and Garitano-Zavala, Á.** (2017). Aerobic performance in tinamous is limited by their small heart. A novel hypothesis in the evolution of avian flight. *Sci. Rep.* **7**, 15964. doi:10.1038/s41598-017-16297-2
- Badr, A., Korajoki, H., Abu-Amra, E.-S., El-Sayed, M. F. and Vornanen, M.** (2018). Effects of seasonal acclimatization on thermal tolerance of inward currents in roach (*Rutilus rutilus*) cardiac myocytes. *J. Comp. Physiol. B Biochem. Syst. Environ. Physiol.* **188**, 255-269. doi:10.1007/s00360-017-1126-1
- Bavis, R. W. and Kilgore, D. L.** (2001). Effects of embryonic CO_2 exposure on the adult ventilatory response in quail: does gender matter? *Respir. Physiol.* **126**, 183-199. doi:10.1016/S0034-5687(01)00206-7
- Bogdanov, K. Y., Ziman, B. D., Spurgeon, H. A. and Lakatta, E. G.** (1995). L- and T-type calcium currents differ in finch and rat ventricular cardiomyocytes. *J. Mol. Cell. Cardiol.* **27**, 2581-2593. doi:10.1006/jmcc.1995.0045
- Bootman, M. D., Higazi, D. R., Coombes, S. and Roderick, H. L.** (2006). Calcium signalling during excitation-contraction coupling in mammalian atrial myocytes. *J. Cell Sci.* **119**, 3915-3925. doi:10.1242/jcs.03223
- Bossen, E. H., Sommer, J. R. and Waugh, R. A.** (1978). Comparative stereology of the mouse and finch left ventricle. *Tissue Cell* **10**, 773-784. doi:10.1016/0040-8166(78)90062-9
- Boukens, B. J. D., Kristensen, D. L., Filogonio, R., Carreira, L. B. T., Sartori, M. R., Abe, A. S., Currie, S., Joyce, W., Conner, J., Opthof, T. et al.** (2019). The electrocardiogram of vertebrates: evolutionary changes from ectothermy to endothermy. *Prog. Biophys. Mol. Biol.* **144**, 16-29. doi:10.1016/j.pbiomolbio.2018.08.005
- Brotto, M. and Creazzo, T. L.** (1996). Ca^{2+} transients in embryonic chick heart: contributions from Ca^{2+} channels and the sarcoplasmic reticulum. *Am. J. Physiol. Heart Circ. Physiol.* **270**, H518-H525. doi:10.1152/ajpheart.1996.270.2.H518
- Cavalié, A., McDonald, T. F., Pelzer, D. and Trautwein, W.** (1985). Temperature-induced transitory and steady-state changes in the calcium current of guinea pig ventricular myocytes. *Pflügers Arch. Eur. J. Physiol.* **405**, 294-296. doi:10.1007/BF00582574
- Creazzo, T. L., Burch, J. and Godt, R. E.** (2004). Calcium buffering and excitation-contraction coupling in developing avian myocardium. *Biophys. J.* **86**, 966-977. doi:10.1016/S0006-3495(04)74172-7
- Cros, C., Sallé, L., Warren, D. E., Shiels, H. A. and Brette, F.** (2014). The calcium stored in the sarcoplasmic reticulum acts as a safety mechanism in rainbow trout heart. *Am. J. Physiol. Integr. Comp. Physiol.* **307**, R1493-R1501. doi:10.1152/ajpregu.00127.2014
- Delbridge, L. M., Bassani, J. W. and Bers, D. M.** (1996). Steady-state twitch Ca^{2+} fluxes and cytosolic Ca^{2+} buffering in rabbit ventricular myocytes. *Am. J. Physiol. Cell Physiol.* **270**, C192-C199. doi:10.1152/ajpcell.1996.270.1.C192
- Dibb, K. M., Clarke, J. D., Eisner, D. A., Richards, M. A. and Trafford, A. W.** (2013). A functional role for transverse (t -) tubules in the atria. *J. Mol. Cell. Cardiol.* **58**, 84-91. doi:10.1016/j.yjmcc.2012.11.001
- Dzialowski, E. and Crossley, D.** (2015). The cardiovascular system. In *Sturkie's Avian Physiology* (ed. C. G. Scanes), pp. 199-201. San Diego: Academic Press.
- Fabiato, A.** (1983). Calcium-induced release of calcium from the cardiac sarcoplasmic reticulum. *Am. J. Physiol. Cell Physiol.* **245**, C1-C14. doi:10.1152/ajpcell.1983.245.1.c1
- Fabiato, A.** (1985). Effects of ryanodine in skinned cardiac cells. *Fed. Proc.* **44**, 2970-2976.
- Filatova, T. S., Abramochkin, D. V. and Shiels, H. A.** (2019). Thermal acclimation and seasonal acclimatization: a comparative study of cardiac response to prolonged temperature change in shorthorn sculpin. *J. Exp. Biol.* **222**, jeb202242. doi:10.1242/jeb.202242
- Forbes, M. S., Mock, O. B. and Van Niel, E. E.** (1990). Ultrastructure of the myocardium of the least shrew, *Cryptotis parva* Say. *Anat. Rec.* **226**, 57-70. doi:10.1002/ar.1092260108
- Franzini-Armstrong, C., Protasi, F. and Ramesh, V.** (1999). Shape, size, and distribution of Ca^{2+} release units and couplings in skeletal and cardiac muscles. *Biophys. J.* **77**, 1528-1539. doi:10.1016/S0006-3495(99)77000-1
- Franzini-Armstrong, C., Protasi, F. and Tijksens, P.** (2005). The assembly of calcium release units in cardiac muscle. *Ann. N. Y. Acad. Sci.* **1047**, 76-85. doi:10.1196/annals.1341.007
- Galli, G. L. J., Lipnick, M. S., Shiels, H. A. and Block, B. A.** (2011). Temperature effects on Ca^{2+} cycling in scombrid cardiomyocytes: a phylogenetic comparison. *J. Exp. Biol.* **214**, 1068-1076. doi:10.1242/jeb.048231
- Galli, G. L. J., Taylor, E. W. and Shiels, H. A.** (2006). Calcium flux in turtle ventricular myocytes. *Am. J. Physiol. Integr. Comp. Physiol.* **291**, R1781-R1789. doi:10.1152/ajpregu.00421.2006
- Galli, G. L. J., Warren, D. E. and Shiels, H. A.** (2009). Ca^{2+} cycling in cardiomyocytes from a high-performance reptile, the varanid lizard (*Varanus exanthematicus*). *Am. J. Physiol. Integr. Comp. Physiol.* **297**, R1636-R1644. doi:10.1152/ajpregu.00381.2009
- Ginsburg, K. S., Weber, C. R. and Bers, D. M.** (1998). Control of maximum sarcoplasmic reticulum Ca load in intact ferret ventricular myocytes: effects of thapsigargin and isoproterenol. *J. Gen. Physiol.* **111**, 491-504. doi:10.1085/jgp.111.4.491
- Grubb, B. R.** (1983). Allometric relations of cardiovascular function in birds. *Am. J. Physiol. Heart Circ. Physiol.* **245**, H567-H572. doi:10.1152/ajpheart.1983.245.4.h567
- Gwathmey, J. K., Kim, C. S., Hajjar, R. J., Khan, F., DiSalvo, T. G., Matsumori, A. and Bristow, M. R.** (1999). Cellular and molecular remodeling in a heart failure model treated with the β -blocker carvedilol. *Am. J. Physiol. Heart Circ. Physiol.* **276**, H1678-H1690. doi:10.1152/ajpheart.1999.276.5.H1678
- Hadley, R. W. and Lederer, W. J.** (1991). Ca^{2+} and voltage inactivate Ca^{2+} channels in guinea-pig ventricular myocytes through independent mechanisms. *J. Physiol.* **444**, 257-268. doi:10.1113/jphysiol.1991.sp018876
- Hatano, S., Yamashita, T., Sekiguchi, A., Iwasaki, Y., Nakazawa, K., Sagara, K., Iinuma, H., Aizawa, T. and Fu, L.-T.** (2006). Molecular and electrophysiological differences in the L-type Ca^{2+} channel of the atrium and ventricle of rat hearts. *Circ. J.* **70**, 610-614. doi:10.1253/circj.70.610
- Haverinen, J. and Vornanen, M.** (2009). Comparison of sarcoplasmic reticulum calcium content in atrial and ventricular myocytes of three fish species. *Am. J. Physiol. Regul. Integr. Comp. Physiol.* **297**, R1180-R1187. doi:10.1152/ajpregu.00022.2009
- Haworth, T. E., Haverinen, J., Shiels, H. A. and Vornanen, M.** (2014). Electrical excitability of the heart in a Chondrostei fish, the Siberian sturgeon (*Acipenser baerii*). *Am. J. Physiol. Integr. Comp. Physiol.* **307**, R1157-R1166. doi:10.1152/ajpregu.00253.2014
- Herve, J. C., Yamaoka, K., Twist, V. W., Powell, T., Ellory, J. C. and Wang, L. C.** (1992). Temperature dependence of electrophysiological properties of guinea pig and ground squirrel myocytes. *Am. J. Physiol. Regul. Integr. Comp. Physiol.* **263**, R177-R184. doi:10.1152/ajpregu.1992.263.1.R177
- Hicks, J. W. and Wang, T.** (2012). The functional significance of the reptilian heart: new insights into an old question. In *Ontogeny and Phylogeny of the Vertebrate Heart* (ed. D. Sedmera and T. Wang), pp. 207-227. New York: Springer.
- Hillman, S. S. and Hedrick, M. S.** (2015). A meta-analysis of *in vivo* vertebrate cardiac performance: implications for cardiovascular support in the evolution of endothermy. *J. Exp. Biol.* **218**, 1143-1150. doi:10.1242/jeb.118372
- Hirakow, R.** (1970). Ultrastructural characteristics of the mammalian and sauropsidan heart. *Am. J. Cardiol.* **25**, 195-203. doi:10.1016/0002-9149(70)90579-5
- Hove-Madsen, L., Llach, A. and Tort, L.** (2001). The function of the sarcoplasmic reticulum is not inhibited by low temperatures in trout atrial myocytes. *Am. J. Physiol. Regul. Integr. Comp. Physiol.* **281**, R1902-R1906. doi:10.1152/ajpregu.2001.281.6.R1902
- Isenberg, G. and Klockner, U.** (1982). Calcium tolerant ventricular myocytes prepared by preincubation in a 'KB medium'. *Pflügers Arch. Eur. J. Physiol.* **395**, 6-18. doi:10.1007/BF00584963
- Jackson, C. A. W., Kingston, D. J. and Hemsley, L. A.** (1972). A total mortality survey of nine batches of broiler chickens. *Aust. Vet. J.* **48**, 481-487. doi:10.1111/j.1751-0813.1972.tb02303.x
- Jensen, B., van den Berg, G., van den Doel, R., Oostra, R.-J., Wang, T. and Moorman, A. F. M.** (2013b). Development of the hearts of lizards and snakes and perspectives to cardiac evolution. *PLoS ONE* **8**, e63651. doi:10.1371/journal.pone.0063651
- Jensen, B., Wang, T., Christoffels, V. M. and Moorman, A. F. M.** (2013a). Evolution and development of the building plan of the vertebrate heart. *Biochim. Biophys. Acta Mol. Cell Res.* **1833**, 783-794. doi:10.1016/j.bbamcr.2012.10.004

- Julian, R. J.** (1987). Are we growing them too fast? Ascites in meat-type chickens. *Highlights Agric. Res. Ont.* **10**, 27-30.
- Julian, R. J.** (1998). Rapid growth problems: ascites and skeletal deformities in broilers. *Poult. Sci.* **77**, 1773-1780. doi:10.1093/ps/77.12.1773
- Junker, J., Sommer, J. R., Sar, M. and Meissner, G.** (1994). Extended junctional sarcoplasmic reticulum of avian cardiac muscle contains functional ryanodine receptors. *J. Biol. Chem.* **269**, 1627-1634.
- Kawano, S. and DeHaan, R. L.** (1991). Developmental changes in the calcium currents in embryonic chick ventricular myocytes. *J. Membr. Biol.* **120**, 17-28. doi:10.1007/BF01868587
- Kim, C. S., Davidoff, A. J., Maki, T. M., Doye, A. A. and Gwathmey, J. K.** (2000). Intracellular calcium and the relationship to contractility in an avian model of heart failure. *J. Comp. Physiol. B Biochem. Syst. Environ. Physiol.* **170**, 295-306. doi:10.1007/s00360000103
- Kitchens, S. A., Burch, J. and Creazzo, T. L.** (2003). T-type Ca^{2+} current contribution to Ca^{2+} -induced Ca^{2+} release in developing myocardium. *J. Mol. Cell. Cardiol.* **35**, 515-523. doi:10.1016/S0022-2828(03)00075-0
- Loughrey, C. M., Smith, G. L. and MacEachern, K. E.** (2004). Comparison of Ca^{2+} release and uptake characteristics of the sarcoplasmic reticulum in isolated horse and rabbit cardiomyocytes. *Am. J. Physiol. Circ. Physiol.* **287**, H1149-H1159. doi:10.1152/ajpheart.00060.2004
- Mackenzie, L., Roderick, H. L., Berridge, M. J., Conway, S. J. and Bootman, M. D.** (2004). The spatial pattern of atrial cardiomyocyte calcium signalling modulates contraction. *J. Cell Sci.* **117**, 6327-6337. doi:10.1242/jcs.01559
- Magwood, S. E. and Bray, D. F.** (1962). Disease condition of turkey poults characterized by enlarged and rounded hearts. *Can. J. Comp. Med. Vet. Sci.* **26**, 268-272.
- Marcus, N. C. and Fozzard, H.** (1981). Tetrodotoxin sensitivity in the developing and adult chick heart. *J. Mol. Cell. Cardiol.* **13**, 335-340. doi:10.1016/0022-2828(81)90322-9
- Mitrokhin, V., Filatova, T., Shim, A., Bilichenko, A., Abramochkin, D., Kamkin, A. and Mladenov, M.** (2019). L-type Ca^{2+} channels' involvement in IFN- γ -induced signaling in rat ventricular cardiomyocytes. *J. Physiol. Biochem.* **75**, 109-115. doi:10.1007/s13105-019-00662-y
- Naganobu, K. and Hagio, M.** (2000). Dose-related cardiovascular effects of isoflurane in chickens during controlled ventilation. *J. Vet. Med. Sci.* **62**, 435-437. doi:10.1292/jvms.62.435
- Nain, S., Ling, B., Alcorn, J., Wojnarowicz, C. M., Laarveld, B. and Olkowski, A. A.** (2008). Biochemical factors limiting myocardial energy in a chicken genotype selected for rapid growth. *Comp. Biochem. Physiol. A Mol. Integr. Physiol.* **149**, 36-43. doi:10.1016/j.cbpa.2007.10.001
- Negretti, N., Varro, A. and Eisner, D. A.** (1995). Estimate of net calcium fluxes and sarcoplasmic reticulum calcium content during systole in rat ventricular myocytes. *J. Physiol.* **486**, 581-591. doi:10.1113/jphysiol.1995.sp020836
- Ogura, T., Shuba, L. M. and McDonald, T. F.** (1999). L-type Ca^{2+} current in guinea pig ventricular myocytes treated with modulators of tyrosine phosphorylation. *Am. J. Physiol. Circ. Physiol.* **276**, H1724-H1733. doi:10.1152/ajpheart.1999.276.5.H1724
- Park, S.-J., Min, S.-H., Kang, H.-W. and Lee, J.-H.** (2015). Differential zinc permeation and blockade of L-type Ca^{2+} channel isoforms Cav1.2 and Cav1.3. *Biochim. Biophys. Acta Biomembr.* **1848**, 2092-2100. doi:10.1016/j.bbamem.2015.05.021
- Perni, S., Iyer, V. R. and Franzini-Armstrong, C.** (2012). Ultrastructure of cardiac muscle in reptiles and birds: optimizing and/or reducing the probability of transmission between calcium release units. *J. Muscle Res. Cell Motil.* **33**, 145-152. doi:10.1007/s10974-012-9297-6
- Richards, M. A., Clarke, J. D., Saravanan, P., Voigt, N., Dobrev, D., Eisner, D. A., Trafford, A. W. and Dibb, K. M.** (2011). Transverse tubules are a common feature in large mammalian atrial myocytes including human. *Am. J. Physiol. Heart Circ. Physiol.* **301**, H1996-H2005. doi:10.1152/ajpheart.00284.2011
- Ringer, R. K.** (1968). Blood pressure of Japanese and bobwhite quail. *Poult. Sci.* **47**, 1602-1604. doi:10.3382/ps.0471602
- Ruben, J.** (1995). The evolution of endothermy in mammals and birds: from physiology to fossils. *Annu. Rev. Physiol.* **57**, 69-95. doi:10.1146/annurev.ph.57.030195.000441
- Sarantopoulos, C., McCallum, J. B., Kwok, W.-M. and Hogan, Q.** (2004). β -Escin diminishes voltage-gated calcium current rundown in perforated patch-clamp recordings from rat primary afferent neurons. *J. Neurosci. Methods* **139**, 61-68. doi:10.1016/j.jneumeth.2004.04.015
- Sham, J. S.** (1997). Ca^{2+} release-induced inactivation of Ca^{2+} current in rat ventricular myocytes: evidence for local Ca^{2+} signalling. *J. Physiol.* **500**, 285-295. doi:10.1113/jphysiol.1997.sp022020
- Sheard, T. M. D., Kharche, S. R., Pinali, C. and Shiels, H. A.** (2019). 3D ultrastructural organisation of calcium release units in the avian sarcoplasmic reticulum. *J. Exp. Biol.* **222**, jeb197640. doi:10.1242/jeb.197640
- Shiels, H. A. and Galli, G. L. J.** (2014). The sarcoplasmic reticulum and the evolution of the vertebrate heart. *Physiology* **29**, 456-469. doi:10.1152/physiol.00015.2014
- Shiels, H. A. and Sitsapesan, R.** (2015). Is there something fishy about the regulation of the ryanodine receptor in the fish heart? *Exp. Physiol.* **100**, 1412-1420. doi:10.1113/EP085136
- Shiels, H. A., Blank, J. M., Farrell, A. P. and Block, B. A.** (2004). Electrophysiological properties of the L-type Ca^{2+} current in cardiomyocytes from bluefin tuna and Pacific mackerel. *Am. J. Physiol. Integr. Comp. Physiol.* **286**, R659-R668. doi:10.1152/ajpregu.00521.2003
- Shiels, H. A., Vornanen, M. and Farrell, A. P.** (2000). Temperature dependence of L-type Ca^{2+} channel current in atrial myocytes from rainbow trout. *J. Exp. Biol.* **203**, 2771-2780.
- Shiels, H. A., Vornanen, M. and Farrell, A. P.** (2002). Temperature dependence of cardiac sarcoplasmic reticulum function in rainbow trout myocytes. *J. Exp. Biol.* **205**, 3631-3639.
- Shimoni, Y. and Banno, H.** (1993). Thyroxine effects on temperature dependence of ionic currents in single rabbit cardiac myocytes. *Am. J. Physiol. Heart Circ. Physiol.* **265**, H1875-H1883. doi:10.1152/ajpheart.1993.265.6.H1875
- Snelling, E. P., Taggart, D. A., Maloney, S. K., Farrell, A. P., Leigh, C. M., Waterhouse, L., Williams, R. and Seymour, R. S.** (2015). Scaling of left ventricle cardiomyocyte ultrastructure across development in the kangaroo *Macropus fuliginosus*. *J. Exp. Biol.* **218**, 1767-1776. doi:10.1242/jeb.119453
- Sommer, J. R. and Jennings, R. B.** (1986). Ultrastructure of cardiac muscle. In *Heart and Cardiovascular System, Scientific Foundations* (ed. H. A. Fozzard, R. B. Jennings, E. Haber, A. M. Katz and H. E. Morgan), pp. 61-100. NY: Raven Press.
- Stern, M. D., Pizarro, G. and Ríos, E.** (1997). Local control model of excitation-contraction coupling in skeletal muscle. *J. Gen. Physiol.* **110**, 415-440. doi:10.1085/jgp.110.4.415
- Tanaka, H., Takagi, N. and Shigenobu, K.** (1995). Difference in excitation-contraction mechanisms between atrial and ventricular myocardia of hatched chicks. *Gen. Pharmacol.* **26**, 45-49. doi:10.1016/0306-3623(94)00167-L
- Valance, D., Després, G., Richard, S., Constantin, P., Mignon-Grasteau, S., Leman, S., Boissy, A., Faure, J.-M. and Leterrier, C.** (2008). Changes in heart rate variability during a tonic immobility test in quail. *Physiol. Behav.* **93**, 512-520. doi:10.1016/j.physbeh.2007.10.011
- Varro, A., Negretti, N., Hester, S. B. and Eisner, D. A.** (1993). An estimate of the calcium content of the sarcoplasmic reticulum in rat ventricular myocytes. *Pflügers Arch. Eur. J. Physiol.* **423**, 158-160. doi:10.1007/BF00374975
- Venetucci, L. A., Trafford, A. W., Díaz, M. E., O'Neill, S. C. and Eisner, D. A.** (2006). Reducing ryanodine receptor open probability as a means to abolish spontaneous Ca^{2+} release and increase Ca^{2+} transient amplitude in adult ventricular myocytes. *Circ. Res.* **98**, 1299-1305. doi:10.1161/01.RES.0000222000.35500.65
- Vornanen, M.** (1997). Sarcolemmal Ca influx through L-type Ca channels in ventricular myocytes of a teleost fish. *Am. J. Physiol. Regul. Integr. Comp. Physiol.* **272**, R1432-R1440. doi:10.1152/ajpregu.1997.272.5.R1432
- Vornanen, M., Hassinen, M. and Haverinen, J.** (2011). Tetrodotoxin sensitivity of the vertebrate cardiac Na^{+} current. *Mar. Drugs* **9**, 2409-2422. doi:10.3390/md9112409
- Vornanen, M., Stevens, E. D., Farrell, A. P. and Graham, J. B.** (1998). L-type Ca^{2+} current in fish cardiac myocytes: effects of thermal acclimation and beta-adrenergic stimulation. *J. Exp. Biol.* **201**, 533-547.
- Walden, A. P., Dibb, K. M. and Trafford, A. W.** (2009). Differences in intracellular calcium homeostasis between atrial and ventricular myocytes. *J. Mol. Cell. Cardiol.* **46**, 463-473. doi:10.1016/j.yjmcc.2008.11.003
- Wilson, W. O.** (1972). A review of the physiology of *Coturnix* (Japanese quail). *World Poult. Sci. J.* **28**, 413-429. doi:10.1079/WPS19720019
- Xu, X. and Best, P. M.** (1992). Postnatal changes in T-type calcium current density in rat atrial myocytes. *J. Physiol.* **454**, 657-672. doi:10.1113/jphysiol.1992.sp019285